A Comprehensive Look at the Electromagnetics of High Field MRI

T. S. Ibrahim[1], C. Mitchell[2], R. Abraham[1], P. Schmalbrock[3]

[1]Electrical and Computer Engineering, University of Oklahoma, Norman, OK, United States, [2]Radiology, Uniformed Services University of the Health Sciences, Bethesda, MD, United States, [3]Radiology, Ohio State University, Columbus, OH, United States

INTRODUCTIONS: With the increasing number of ultra high field (UHF) whole-body MRI systems, the need for robust and versatile radiofrequency (RF) coils that enhance the advantages of these systems is evident. Advancing UHF MRI RF technology to achieve the needed RF coils requires a clear understanding of the operation of these coils when they are loaded. In this work, we explore the TEM resonator [1]. Using experiments and numerical modeling, we will address 2 critical questions associated with the modes produced by the loaded TEM coil, namely 1) what kind of global (across the sample) and local (at a single voxel) polarization they possess and 2) the extent to which their field distributions (excite and receive) differ from those associated with the idealized transverse electromagnetic modes.

METHODS: The RF coil was analyzed both numerically and experimentally. The numerical studies were performed by modeling TEM resonator and the phantom using the FDTD method. Experimental verification of the studies were the performed, using an 18.5 cm diameter sphere containing 0.125 M NaCl, imaged using a 16-strut TEM resonator excited from a single drive port and tuned to the coil's standard mode of operation. GRE imaging was performed on the 8 Tesla whole-body scanner and B_1^+ (excite) and B_1^- (receive) fields were extracted from the images. Fig. 1 shows B_1^+ field distribution obtained 1) experimentally (left) at 8 Tesla for the spherical phantom 2) utilizing the FDTD model for the same conditions as experiment (middle) and for an empty coil (right).

RESULTS: Detailed analysis regarding the polarization of the fields within the empty and loaded was performed. Fig. 2 displays the FDTD calculated polarization vectors for the coil's standard mode of operation across a central axial slice at a single snapshot in time and in a local (close-up) 16 mm^2 area at multiple time snapshots distributed throughout a complete 2π cycle. The intensities of the polarization vectors are represented by the lengths of the arrows and their directions are represented by the arrow tips. The results are obtained for the TEM resonator under two loading conditions: loaded (bottom row) and empty (top row). The coil was linearly excited and numerically tuned to 340 MHz. The data in the unloaded coil plots are shown in an axial circular area in the central plane of the coil; this area has the same size and is in the same location as the displayed loaded case.

When examining the empty coil results, one can easily see that the polarization vectors closely follow what is analytically obtained with circuit theories [2]. The results demonstrate that the direction and the intensity for all the polarization vectors are nearly identical across the slice. Moreover, when examining the local empty-coil polarization vector at multiple time snapshots, it can be clearly seen that the two displayed polarization vectors are linearly polarized; i.e. they are always pointing in the +/- 45° direction with respect to the ***x*** or ***y*** axes. Therefore, for the empty coil, the mode of interest 1) produces a linearly polarized field in the bulk of the coil, and 2) possesses a uniform polarization direction and intensity across the operating region of the coil.

The behavior of the polarization vectors in the loaded coil, however, is quite different than what is observed in the empty coil. The whole-slice polarization data clearly shows that the intensities of the polarization vectors are highly non-uniform across the slice (except in the central region of the slice); this, of course, will lead to non-uniform B_1^+ and B_1^- fields. The inhomogeneity of the magnitude does not by itself, however, provide all relevant information regarding the polarization of these fields. The multiple time snapshots in the loaded coil reveal important results regarding this issue. Within the 16 mm^2 area shown in Fig. 2, the two displayed vectors possess 2 different types of polarization: linear (the tips of the vectors trace a line at all time snapshots) and elliptical (the tips of the vectors trace an ellipse at all the snapshots). Therefore, linear (1-port) excitation at UHF head MRI will result in linearly polarized fields in some regions of the load but not in the entire volume of the load. This in turn will result in a loss of circular polarization during 2-port quadrature excitation. Hence, both the non-uniformity of the magnitudes of the electromagnetic fields produced by the coil's currents and the loss of linear/circular polarization in some regions of the load are attributing to the inhomogeneities of the B_1^+ and B_1^- fields.

To further describe the polarization distribution within the coil, the magnetic field at every voxel in the phantom was classified as follows (shown in Fig. 3): **Lin**ear Polarization: $\xi \le 0.1$, **E**lliptical Polarization: $0.1 < \xi \le 0.9$, and **C**ircular Polarization: $\xi > 0.9$, where $\xi \equiv abs(B_1^+ Intensity - B_1^- Intensity) / max(B_1^+ Intensity, B_1^- Intensity)$. Note for Elliptical and Circular Polarizations, **CW** is associated with $B_1^+ Intensity > B_1^- Intensity$ and **CCW** is associated with $B_1^+ Intensity < B_1^- Intensity$. Also, the field intensities were classified as follows (also shown in Fig. 3): **H**igh: $Intensity > 0.66 \times Maximum$ (describes 46.1% of the total phantom volume), **M**edium: $0.33 \times Maximum < Intensity \le 0.66 \times Maximum$ (describes 53.6% of the total phantom volume), and **L**ow: $Intensity \le 0.33 \times Maximum$ (describes 0.6% of the total phantom volume), where $Maximum = max_{phantom}(B_1^+ Intensity, B_1^- Intensity)$ and $Intensity = average_{voxel}(B_1^+ Intensity, B_1^- Intensity)$ for Linear and $Intensity = max_{voxel}(B_1^+ Intensity, B_1^- Intensity)$ for Circular and Elliptical Polarizations. The spatial locations and the dimensions of these classifications categories in the phantom are shown in Fig 3.

OBSERVATIONS AND CONCLUSIONS: The results demonstrate the accuracy of the developed numerical system in predicting the performance of the resonator. It is shown that for the typical mode of operation in a linearly excited TEM resonator loaded with a head-sized spherical phantom filled with 0.125 NaCl, the following four observations can be made: (1) In the central volume of the coil/phantom, the region near the drive port, and the region opposite to the drive port, the presence of the high intensity and comparable B_1^+ and B_1^- fields is due to the presence of high intensity linearly polarized fields. (2) Surrounding the central bright region of the coil/phantom, the comparable B_1^+ and B_1^- fields of intermediate intensity are due to the presence of intermediate intensity linearly polarized fields. (3) The difference in the relative intensities of the B_1^+ and B_1^- fields at the same location is due to the existence of elliptical polarization. Also, linearly and elliptically polarized fields can exist at locations within close proximity. Finally, the elliptically polarized fields do not rotate in the same sense and can possess either a CW or CCW sense of rotation. (4) If severe lack of signal is observed in UHF MRI head-size experiments, it can only be attributed to a lack of intensity of the B_1^+ field or the B_1^- field, but not of both. (Since the geometry of the object to be imaged as well as its diamagnetic and conductive properties will affect the final image, it is expected that the spatial patterns of B_1^+ and B_1^- fields will be different in brain than in the spherical phantom shown in this work.)

REFERNCES:

1. Vaughan, J. T., et al. High frequency volume coils for clinical NMR imaging and spectroscopy. *MRM*, **32**, pp. 206-218, 1994.

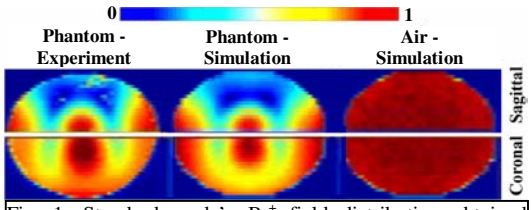

Fig. 1: Standard mode's B_1^+ field distribution obtained experimentally at 8 Tesla with a TEM resonator loaded with a 0.125 NaCl M-filled phantom and using FDTD model for the same conditions as experiment and for an empty coil.

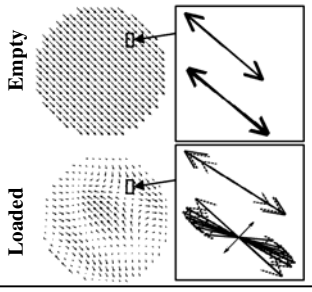

Fig. 2: FDTD calculated polarization vectors in a whole-slice *(at a single snapshot in time)* and locally *(at many time snapshots)* for the coil's standard mode of operation.

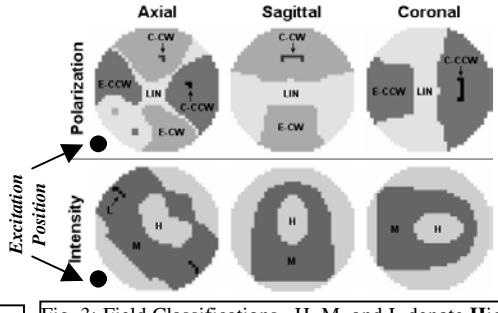

Fig. 3: Field Classifications. H, M, and L denote **H**igh, **M**edium and **L**ow intensities. Lin, C, and E denote **Lin**ear, **C**ircular, and **E**lliptical polarization. CW and CCW denote **C**lock**W**ise and **C**ounter **CW** rotation.